Proceedings of Nuclear and Emerging Technologies for Space 2009
Atlanta, GA, June 14-19, 2009
Paper 203381

ADVANCES IN DESIGN AND MODELING OF THE REACTOR CORE OF OPUS

A. Lokhov, S. Pascal, N. Jonquères
CEA Saclay, DEN, DM2S, F-91191 Gif-sur-Yvette, France
Tel: +33 169084637, Fax: +33 169089935, Email: alexey.lokhov@cea.fr

Abstract – *Optimized Power Unit for Spacecraft (OPUS) is a space electrogenerating nuclear reactor for the range of 100-500 kW_e that has been developed at CEA since 2003. OPUS is a fast spectrum high-temperature gas-cooled reactor concept coupled to a direct Brayton energy conversion cycle. The OPUS fuel consists of uranium dioxide BISO particles distributed in a carbon matrix, enriched to 93% ^{235}U. The core operation is performed by changing the radial leakage factor using twelve mobile beryllium side shutters. In this paper we present the recent advances in core design and modeling.*

I. INTRODUCTION

Since 2003, CEA has been developing a conceptual design of a Nuclear Power Station (NPS) for long space exploration missions. The main project goal consists of designing an evolutionary system capable of delivering 100 kW of electric power in the basic version and up to 500 kW in advanced one. The desired operational full-power lifetime is 2000 days, and the design is based on available nuclear technologies or on those being developed in the framework of the Generation IV Forum.

The resulting project[1] is called OPUS (an acronym for Optimized Power Unit for Spacecraft). OPUS uses a fast spectrum high-temperature gas-cooled reactor (cf. Fig. 1 and TABLE I) coupled to an energy conversion system based on the Brayton cycle. The coolant is a He-Xe mixture with a molecular weight of 85 g/mol.

The reactor is fueled with GBR4 two-layer coated particles (BISO) distributed in a carbon matrix. The kernel of the BISO particles is made of uranium dioxide, enriched to 93% in ^{235}U. The vessel of the core consists of four hydraulically independent parts each containing 63 hexagonal fuel elements.

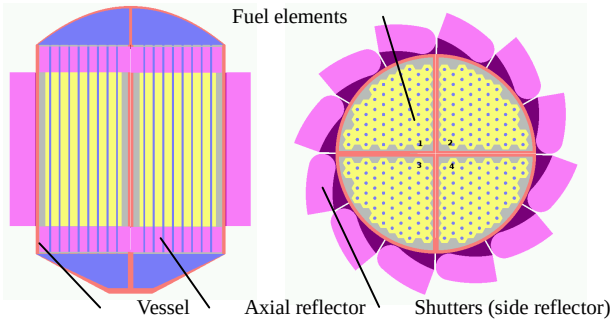

Fig. 1 Radial and axial sections of the core of OPUS.

The axial beryllium-oxide reflectors are positioned inside the vessel. The operation of the reactor is performed by twelve mobile metallic-beryllium shutters constituting the side reflector. Thus, OPUS is operated by changing the neutron leakage factor of the core.

The energy conversion system of OPUS includes two independent loops corresponding to the pairs 1-4 and 2-3 of the quarters or the core (cf. Fig. 1). Each conversion loop consists of a turbocharger/turbine part, heat exchanger-recuperator, generator and radiator.

TABLE I

General characteristics of OPUS

Electrical power	100-500 kW
Thermal power	245-1725 kW
Coolant type	He-Xe, 85 g/mol
Fuel type	Graphite matrix with coated particles
-matrix type	IG-110 graphite
-particle type	BISO GBR4, ∅1.40 mm
-fissile kernel	UO_2 (93% of ^{235}U), ∅0.85 mm
-filling fraction	45%
Uranium masse	193 kg
Reflectors	
- axial	8cm of BeO
- side	8cm of Be
Vessel	Nb1Zr alloy
-thickness	1cm
Inlet core temperature	880 K
Outlet core temperature	1300 K
Coolant flow rate	3.6 kg/s
Radiator	Two-side inconel radiator
-Area	80 m^2
-inlet gas temperature	550 K
-outlet gas temperature	350 K
Total system mass	2400 kg
Specific mass	24 kg/KW

The radiator is the largest part of the system. It is particularly true for the systems based on the gas-turbine mode of conversion because the radiator inlet temperature

is limited by the maximum allowed turbine temperature (of about 1500 K). In the current version of OPUS the total area of the inconel two-sided radiator is 80 m^2 for the basic 100 kW version.

The radiological protection is insured by a three-layer shield including 4 cm of tungsten, 60 cm of LiH in a titanium alloy container and 0.5 cm of tungsten on the edge. The lithium is enriched to 50% in ^{7}Li. This shield guarantees the level of neutron radiation below 10^{12} n/cm^2 and the gamma-ray radiation below 5000 Gy for the payload at 20 m behind the core.

In the following sections we present the main neutron-physical and mechanical characteristics of the OPUS core. Next, the accidental situations that could arise in case of rocket launch failure are considered. Last, the thermomechanical aspects and modeling are presented.

II. NEUTRON-PHYSICAL CHARACERISTICS OF THE CORE OF OPUS

The neutron-physical characteristics relevant to the present stage of development of the project include the core reactivity in various nominal and accidental situations, reactivity decrease with burn-up, the values of the temperature coefficients and some kinetic parameters.

Two models were developed in order to obtain these characteristics. The first model is used to calculate the infinite medium multiplication constant, the Doppler feedback coefficient and to evaluate the reactivity decrease due to the fuel burn-up. It is based on a determinist solution of the neutron transport equation in two dimensions with the APOLLO2 code[2] using the JEFF 3.1 cross-section library[4] (with 281 energy groups). The calculation geometry is obtained from an exact representation of the hexagonal fuel element with periodical boundary conditions. The randomly distributed BISO particles are described using the double-heterogeneity model implemented[3] in APOLLO2. This model allows for a consistent description of stochastic media starting from an exact initial geometry (the BISO particle in our case). With the help of this cell-model, the bulk characteristics of the fuel element were calculated. The results are summarized in the TABLE II.

TABLE II

The bulk neutron-physical characteristics of OPUS 500KW in normal conditions obtained with APOLLO2

k_∞	1.93257
$\Delta\rho_{BU}$	-0.56 pcm/day (at 500 kW)
$\alpha_{Doppler}$	-0.015 pcm/K
β_{eff}	776 pcm
"r" parameter $\overline{\nu\Sigma_f}/\overline{\xi\Sigma_s}$	0.534

The value of the "r" parameter is quite high and thus the spectrum of OPUS is hard despite large quantity of graphite present in the core, and that the Doppler effect is almost insignificant due to the high enrichment of the fuel in the ^{235}U isotope.

In order to obtain precise core characteristics, a Monte-Carlo three-dimensional modeling was performed with the code Tripoli-4,[5,6] using the ENDF/B-VII cross sections library.[7] The heterogeneity of the fuel was neglected in order to reduce the complexity of the core simulation. The mean free path of a neutron is OPUS core is about 3.5cm, and thus the internal structure of the fuel element may be neglected. A test Monte-Carlo calculation was performed for two descriptions of the fuel: with BISO particles randomly distributed in the matrix and an homogenized medium (cf. Fig. 2). The resulting multiplicative constants are close (within 150 pcm) [1].

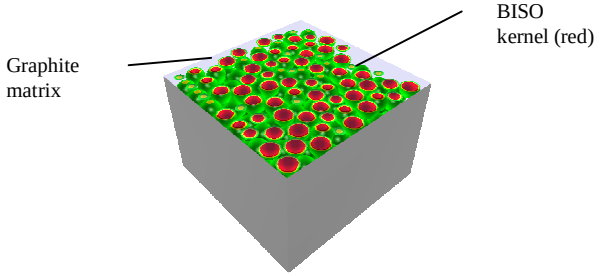

Fig. 2 Detailed description of OPUS fuel with 45%$_{vol}$ filling with BISO particles.

The operational conditions of the core, especially the temperature of different parts, were obtained with the help of the thermomechanical model discussed in Section IV. This model used as input a power distribution calculated on the 'cold' core. As a result, mean temperatures and deformations were evaluated for the fuel and the structures of the reactor. In the TABLE III the results for the core reactivity in operational conditions are summarized (obtained with a 3D core model with homogeneous fuel).

TABLE III

OPUS characteristics in operational conditions

Mean temperature of the fuel	1500 K
Mean temperature of the vessel/reflector	900 K
Mean temperature expansion coefficient	$4.02 \cdot 10^{-6}$ K^{-1}
k_{eff} all shutter closed	1.03999 (σ=9 pcm)
k_{eff} all shutter open	0.93688 (σ=8 pcm)
One shutter efficiency	12 pcm/arc degree

[1] k_{eff} =1.93637 (heterogeneous case) and k_{eff} =1.93746 (homogenized case) with σ<10pcm.

III. SAFETY IN CASE OF LAUNCH FAILURE

In spite of significant improvement of the rocket launch reliability, the probability of failure is still quite important (cf. Fig. 3). It is extremely important to ensure the subcriticality of the reactor no matter the conditions. Depending on the nature of the hypothetical accidental situation, the core could be immersed in water or clay, flooded or not, strongly deformed etc.

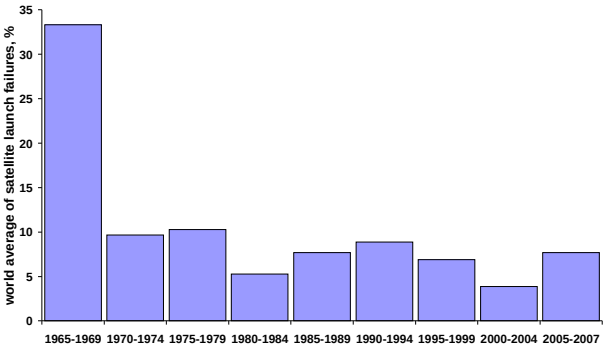

Fig. 3 World average percentage of satellite launch failures[8].

The existing NPS projects use various methods in order to guarantee accidental subcriticality. They include special security rods, thermal neutrons absorbers or fuel element ejection. The use of spectral shift absorbers in OPUS seems problematic because of the important part (around 5%) of thermal-neutron fissions in the core. The solution considered as the simplest consists of separating the core into four parts in an accident scenario. In this section we shall evaluate the reactivity increase in some representative types of accidents and try to evaluate the energy release in hypothetical failure of all safety equipment.

III.A. The impact of deformation

With the help of the Monte-Carlo simulations one can evaluate the increase of the core reactivity in various immersion accident, but the impact of the deformation is extremely difficult to obtain by a direct calculation. However, by considering a maximal compaction (leading to a spherical form) one can get an estimate of the reactivity after the impact.

Writing for the effective multiplication constant

$$k_{eff}^{cyl} = \frac{k_\infty}{1 + L^2 B_{cyl}^2}, \qquad (1)$$

one has after compaction:

$$k_{eff}^{sph} = \frac{k_\infty}{1 + \frac{B_{sph}^2}{B_{cyl}^2}\left(\frac{k_\infty}{k_{eff}^{cyl}} - 1\right)} \approx \frac{k_\infty}{1 + 0.908\left(\frac{k_\infty}{k_{eff}^{cyl}} - 1\right)}. \qquad 2)$$

This formula establishes a relation between the reactivity after deformation and the one before, the latter being accessible via the Monte-Carlo simulations. Note that in the case when prismatic (and not cylindrical) form is being compacted, the formula (2) overestimates the result, because neutron leakage in any prismatic core is higher than the one from a cylindrical core of equal volume (and having the same height). We shall use this result in the next section.

III.B. Reactivity increase in case of immersion of the core

Twelve hypothetical accidental situations were investigated: when the whole OPUS core or one fourth of it falls into the clear water or clay, with or without side reflector and flooded or not by the surrounding medium. The temperature of the water was fixed at 274 K and the composition of the clay is the one of kaolinite[9]: 47% of SiO_2, 39% of Al_2O_3 and 14% of H_2O. The effective multiplication constant obtained using Monte-Carlo simulations are given in the TABLE IV. In the same table the estimated values for corresponding

TABLE IV

Effective multiplication constant for entire OPUS or its parts immersed to water and clay (non deformed case)

falling object	side reflector	Medium	Reactor flooded	k_{eff}	k_{eff}^{sph}
OPUS	present	Water	yes	1.26949 σ=16 pcm	1.311
OPUS	present	Water	not	1.15315 σ=18 pcm	1.198
OPUS	present	Clay	yes	1.19898 σ=16 pcm	1.242
OPUS	present	Clay	not	1.15681 σ=16 pcm	1.201
OPUS	absent	Water	yes	1.19236 σ=15 pcm	1.236
OPUS	absent	Water	not	1.05416 σ=10 pcm	1.100
OPUS	absent	Clay	yes	1.14374 σ=14 pcm	1.188
OPUS	absent	Clay	not	1.09651 σ=9 pcm	1.142
¼OPUS	N/A	Water	yes	0.88863 σ=36 pcm	0.935
¼OPUS	N/A	Water	not	0.76745 σ=13 pcm	0.812
¼OPUS	N/A	Clay	yes	0.83461 σ=9 pcm	0.881
¼OPUS	N/A	Clay	not	0.79644 σ=12 pcm	0.842

compacted cases are given (only significant figures). They are obtained from Eq. (2). As k_{eff}^{sph} is a growing function

of k_∞, one should take the highest possible value among unflooded and water- or clay-flooded situations. Thus all intermediate cases, such as a partly-flooded core, are taken into account. The cell calculations with APOLLO2 showed that the unflooded case yields maximal k_∞.

One finds that when the whole reactor falls in moderating and reflecting medium, the reactivity insertion is extremely high compared to the delayed neutrons reactivity fraction β_{eff}. In the case of one quarter of the core in the same conditions, the fragment remains deeply subcritical.

III.C. Estimating the energy released

Now we consider the hypothetical situation when all safety devices have failed and the worst possible reactivity insertion accident occurs. In order to estimate the energy release following such an accident one can apply the adiabatic model supposing that all the fission energy contributes to the Doppler feedback.

This assumption is valid if the peak power duration is shorter than the time needed to transfer the heat from the kernel of the fuel particle to the surrounding medium. One can show that, for a step insertion of a very big reactivity Δk_0 into a core at very low power, the peak power length is proportional to the ratio Λ / k_0 where Λ is the mean generation time. In our case Δk_0 is close to 0.3 and $\Lambda = 2.6 \cdot 10^{-7}$ s (in the water-flooded case). Thus the power burst time is much shorter than the time characterizing the heat removal from the fissile kernel of the BISO particle (around 10^{-3} s), [10] and the adiabatic model is applicable.

In the framework of the adiabatic model the energy density $E(t)$ released in the burst can be obtained from the point kinetics equation with feedback (the delayed neutrons are neglected):

$$\begin{cases} \dfrac{dP(t)}{dt} = \dfrac{\Delta k_0}{\Lambda} P(t) - \dfrac{\alpha_T}{\Lambda \rho C_p} P(t) \int_0^t P(\tau) d\tau \\ \dfrac{dE(t)}{dt} = P(t) \\ E(0) = 0, \; P(0) \equiv \dfrac{dE(0)}{dt} = P_0 \end{cases} \quad (3)$$

In this equation α_T is the temperature feedback coefficient and ρ, C_p is fuel density and specific heat of the fuel. [2] The initial conditions specify the zero-time energy and power P_0, the latter is due to spontaneous fissions and thus it is very small. This allows one to get a simple expression for the delivered energy:

$$E_{tot} = \frac{2\Delta k_0}{|\alpha_T|} \rho C_p V_{fuel}$$

According to the results obtained with APOLLO2 cell-model, the feedback coefficient α_T is equal to

$$\alpha_T^{water} = -0.26 \text{ pcm/K}$$

in the case when the cell is flooded with water and to

$$\alpha_T^{clay} = -0.10 \text{ pcm/K}$$

in the case of clay. For the non-flooded situation the nominal coefficient ($\alpha_T = -0.015$ pcm/K, cf. TABLE II) was used. The results for the energy released in case of the accidental situation given in TABLE IV are presented in the TABLE V.

TABLE V

Energy release estimations

falling object	side reflector	Medium	Reactor flooded	Energy released, ton of TNT	Mass of Fissioned ^{235}U, kg
OPUS	present	Water	yes	13 t	$6.6 \cdot 10^{-4}$ kg
OPUS	present	Water	not	140 t	$7.1 \cdot 10^{-3}$ kg
OPUS	present	Clay	yes	26 t	$1.3 \cdot 10^{-3}$ kg
OPUS	present	Clay	not	142 t	$7.2 \cdot 10^{-3}$ kg
OPUS	absent	Water	yes	10 t	$5.1 \cdot 10^{-4}$ kg
OPUS	absent	Water	not	71 t	$3.6 \cdot 10^{-3}$ kg
OPUS	absent	Clay	yes	20 t	$1.1 \cdot 10^{-3}$ kg
OPUS	absent	Clay	not	100 t	$5.1 \cdot 10^{-3}$ kg

III.D. Conclusions

The separation of the core into four parts in the case of launch failure ensures subcriticality after immersion and compaction. If the core remains entire after launch failure (highly improbable situation), an explosion of an estimated strength of around 150 tons equivalent TNT could occur, and up to ten grams of fission products released. Although this quantity is limited, such a release is socially inacceptable and to avoid this, a neutron thermal poison (B_4C) is introduced on the external part of the axial reflectors. Thus the neutron poison does not influence the core reactivity in normal conditions, and is available in case of the accident. This last point is under investigation now and will be published elsewhere.

IV. THERMOMECHANICS & THERMOHYDRAULICS OF THE REACTOR CORE

The current design of OPUS is a result of several iterations between neuron-physical and thermomechanical considerations. So, the thermomechanical study is always based on a previous neutronic design, which is currently characterized by a reactor *in one part* (see Fig. 4), unlike the one considered in the previous sections, where it is

[2] These quantities are considered as independent of the fuel temperature.

divided in four parts (see Fig. 1). However, the one-part thermomechanical model *a priori* overestimates the temperatures in the core and thus can be used to obtain the upper bounds of the thermal characteristics of the sectorized design. In this article, the discussed thermomechanical study only deals with the 100 kWe OPUS version.

The thermomechanical design relies on finite element simulations of the thermomechanical fields that occur in the reactor at nominal power. These simulations are carried out with the CEA's finite element software Cast3M[11]. To achieve such simulations, we have to face two main difficulties. First, to determine the mean properties of the fuel elements, which are unknown since the composition of the considered nuclear fuel is part of the design. This led to the development of a homogenization model derived in the published literature[1,14]. Second, the strong heterogeneity of power density and the small size of the reactor require coupled thermal-thermohydraulic simulations to get an accurate estimation of the temperature in the system. In the following, we briefly sum-up the developments carried out on the fuel element modeling since they have been already published[14], and present the finite element simulations achieved to get the temperature and the stresses in the reactor.

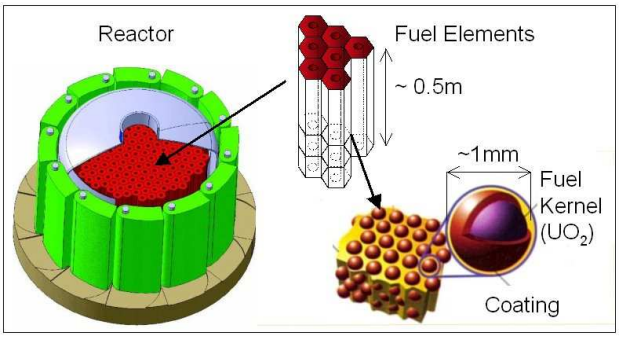

Fig. 4 The different scales of the thermomechanical modeling.

IV.A. Fuel Element Modeling

The ceramic composite constituting the fuel elements is modelled using a homogenization model taken from the literature[12,13]. It provides the effective properties of fuel according to the properties of its components. We then substitute the original heterogeneous media, constituted of fuel particles embedded into a graphite matrix (see Fig. 4), with an equivalent homogeneous media which behaves as the whole. This model also gives an estimate of the mean value of the strains and stresses in each phase of the material. Finally, it was extended to take into account the volume change of the different phases under irradiation by doing an analogy between irradiation-induced strain and thermal expansion. Model validation was achieved by comparing estimations of the fuel properties to average properties obtained by finite element simulations on periodic meshes representing the fuel microstructure[14].

The thermomechanical data applied are mainly taken from the literature. For the UO_2 kernel, the properties depend on the temperature and the neutron fluence[15-17]. For the graphite matrix, we have considered the properties of the fine-grained nuclear graphite (IG-110) involved in the Japanese HTTR project for which a good thermomechanical characterization is available[18]. For the pyrocarbones, the properties are taken from a CEA internal review[19].

We also paid attention to the internal stress state induced during the fuel fabrication. Basic thermoelastic simulations of the different steps of the fabrication process (chemical vapour deposition of pyrocarbon layers on the UO_2 kernel at 1300 °C and hot casting of the mixture of fuel particles and graphite powder at 1800 °C) led to the conclusion that the *UO_2 kernel is mechanically disconnected from the particle layers after fabrication*. Moreover the analysis of the shrinkage and the swelling of the different phases under irradiation shows that this fact remains during the whole duration of a mission (2000 EFDP - Equivalent Full Power Days) if the fuel temperature stays below 1800°C. Finally, this analysis also demonstrates that the mechanical integrity of the particle is insured only if its interface with the graphite matrix can easily fail under irradiation to let its external pyrocarbone layer shrink[1].

IV.B. Coupled Thermal-Thermohydraulic Simulations

The finite element mesh used for the simulations is presented in Fig. 5. The symmetry of the problem allows modeling of just 1/12th of the fissile portion of the reactor. The fuel elements appear in red and the pressure vessel in light blue. In yellow, the "core binder" is a graphite

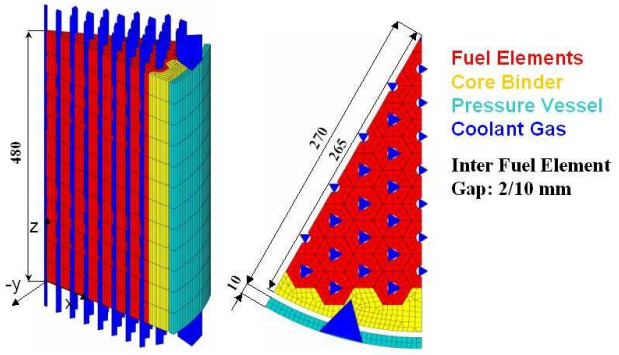

Fig. 5 Finite element mesh of 1/12th of the fissile part of the reactor (dimensions are in millimetres). The mesh of the coolant gas (blue) has been axially expanded to be better shown.

structure which binds the fuel elements. The core binder and the fuel elements represent the fissile part of the reactor core. The cylindrical, empty volume that remains

constitutes the "cold branch" of the coolant path. The coolant gas is modeled by the blue columns of prismatic element mesh. The volume of each blue, finite element column is equal to the coolant channel volume in which it is located in order to properly represent the energy and mass equilibriums. On the figure, this mesh has been axially expanded to be better shown. In the simulations, its height is equal to the one of the other structures.

The main characteristics of the thermohydraulic modeling are the following:

- 1D coolant flow in each channel,
- pressure drop neglected,
- ideal gas law used as coolant state law,
- convective heat exchange ratio given by the Dittus-Boelter analogy.

The boundary conditions are (see also Fig. 6):

- mass flow prescribed at the reactor inlet (cold branch) and at each core channel inlet,
- reactor inlet gas temperature set to 880 K,
- core inlet gas temperature constrained to be equal to the cold branch outlet gas temperature.

For the thermal modeling, the core is considered as a continuous media, *i.e.* the inter-fuel element clearance and the associated temperature jumps are not modeled. The boundary conditions are:

- convective heat exchange with the coolant gas and
- radiant heat exchange between the core and the pressure vessel and from the pressure vessel into space.

The thermal power distribution (see Fig. 6) is derived from

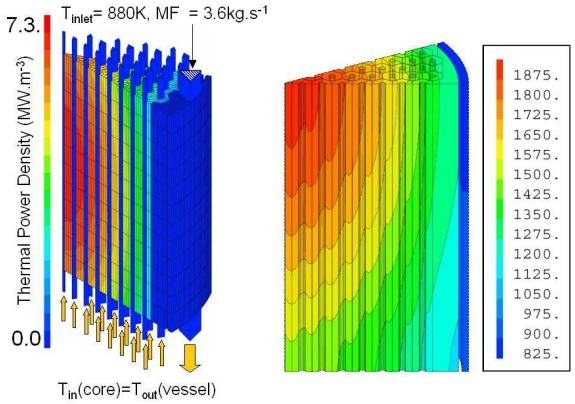

Fig. 6 Thermal power density and main boundary conditions (left) and temperature field (K) at 0 EFPDF (right).

Monte-Carlo neutronic simulations by interpolation with the Bessel and cosine functions in the radial and axial directions, respectively.

The coupling between the thermohydraulic and thermal modeling is simply achieved by solving the two problems alternatively until convergence of both to stationary solutions.

The temperature field obtained in the structures at 0 EFPD is presented at the Fig. 6 and some characteristic temperatures of the coupled solution are given in Table VI. The maximum temperature in the fuel elements is about 1810 K at 0 EFPD. It increases up to 1870K at 2000 EFPD due to the decrease in the graphite thermal conductivity under irradiation. One must notice the strong thermal gradients in the system, especially in the radial direction. It is due both to the strong radial variation of thermal power density, which ranges from 7.3 MW.m^{-3} at the core center down to 2.2 MW.m^{-3} at its periphery, and to the counter-current coolant flow in the reactor.

TABLE VI

Some temperatures (K) in the reactor at 0 and 2000 EFPD

Structures		
Time	0	2000
Maximum of temperature	**1807**	**1870**
Core outlet temperature:		
- center/periphery	1807/1203	1870/1137
- radial gradient (K.m^{-1})	**2279**	**2774**
Hottest fuel element temperature:		
- max./min.	1807/**1427**	1870/**1417**
- axial gradient (K.m^{-1})	790	944
Core binder max./min. temperature	1302/1130	1280/1076
Pressure vessel max./min. temperature	946/906	926/894
Coolant gas		
Maximum of temperature	**1474**	**1491**
Core outlet average gas temperature	1301.6	1302.1
Core outlet gas temperature:		
- max. /min.	1474/1153	1491/1124
- difference hottest-colder channels	321	367
Hottest channel max./min. gas temperature	1474/953	1491/936

These high temperatures are not acceptable, especially since it may be underestimated. Two main reasons lead to this conclusion:

- First, the temperature jumps at the fuel element interface are neglected. If it has little importance at early operating times when the thermal expansion tied them together, their irradiation-induced shrinkage later open a gap between each other that increases the difference of temperature in the radial direction of about 200K.
- Second, coolant flow redistributions over the channels are not taken into account since the mass flow is prescribed at their inlet. Considering the difference of coolant temperature between the channels and the temperature variation of the gas viscosity, it is of evident that such coolant flow redistributions occur.

A solution to balance the temperature in the system may be to consider different channel diameters. However, the last developments in neutronic design presented here above, *i.e.* to split the reactor in four parts (see Fig. 1), lead to a flattened map of power density and then to lower thermal

gradients. Moreover the cooling of the pressure vessel inner surfaces at the center core is also helpful to decrease the maximum temperature.

IV.C. Mechanics

The mechanical modeling is based on the finite element mesh presented Fig. 5, except for the fuel elements that are meshed independently. Contact between fuel elements is then modeled. The mechanical behaviour of the structures is supposed to be linear elastic but the material stiffness is temperature and neutron fluence dependent. Axial displacements are balanced at mid-height of the reactor. The gas pressure (14 MPa) is prescribed on the fuel element and core binder surfaces and on the inner pressure vessel surface. The resultant gas pressure on the lower head pressure vessel surface is also applied. Finally, thermal expansion, irradiation swelling and shrinkage of the materials are modelled.

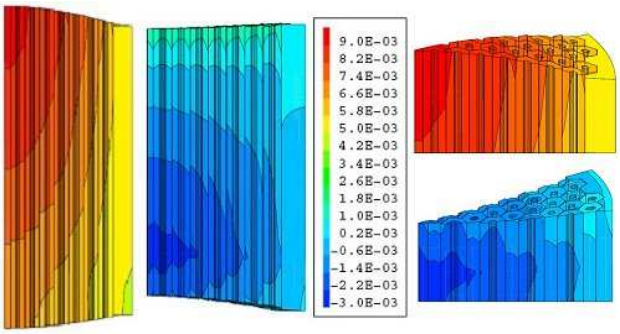

(a) (b)

Fig. 7 Axial strain component (ε_{zz}) on the deformed mesh ($\times 50$ axially) of the reactor at 0 EFPD (a) and at 2000 EFPD (b).

Fig. 7 illustrates the mechanical deformation of the core. It presents the values of the axial strain component at 0 and 2000 EFPD on the deformed mesh of the reactor magnified 50 times on the axial direction. At 2000 EFPD, the irradiation shrinkage of the core is more important than its thermal expansion, making its size smaller than its initial, cold value.

In this problem, the stresses are mainly due to the heterogeneity of thermal or irradiation expansion. Fig. 8 presents the maximum and minimum of the stress components in the matrix phase of the fuel elements versus time, due to the homogenization model of the fuel. The stress is maximum in the axial direction due to the thermal and/or irradiation induced bending of the fuel elements prevented by their surrounding neighbours. The same explanation works for the core binder, except that the orthoradial stress component is also involved since it is a cylinder. This level of stress may be considered too high for the mechanical design of the structures but we assume that the material creep under irradiation will make it acceptable. Finally, the computed stress state of the pressure vessel is very close to one given by usual analytical expressions for an infinite cylinder submitted to an internal pressure, the thermal loading having little influence.

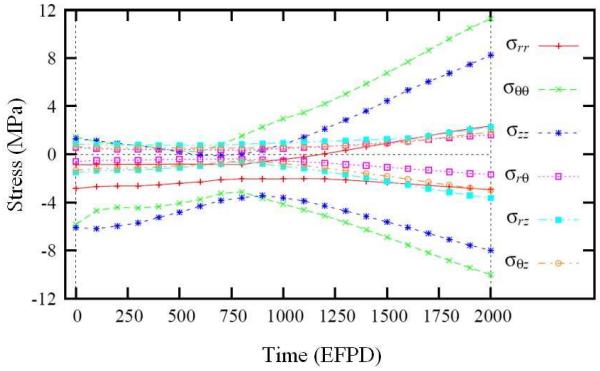

Fig. 8 Maximum and minimum of the stress components in the matrix phase of the fuel elements (MPa) from 0 to 2000 EFPD.

IV.D. Conclusions

Before concluding on the results of the thermo-mechanical study, we first want to outline that the thermal behaviour of such a small, advanced nuclear reactor is not easy to handle and that too coarse calculations on such problems are not able to highlight the technological difficulties they represent. Besides, results on the temperature of a one-part reactor core show that the thermal gradients and the maximum temperature are too important to be really confident on the feasibility of the system, despite the satisfying results concerning the stress-state of the structures. However, solutions exist to make the 100 kWe OPUS version feasible and the latest evolutions on the neutronic design, driven by safety considerations; to divide the reactor in 4 sub-critical parts is certainly one of them. It will be investigated soon.

V. CONCLUSIONS

In the present article, neutron physical and mechanical advances in design of the OPUS nuclear reactor are presented. Particular attention is given to the launch safety system. In case of a major accident, the side reflector is removed and the core is separated in four parts, each being subcritical whatever the conditions.

The maximum energy release in case of failure of the discussed procedure was calculated in the framework of an adiabatic model. For this hypothetical case, the explosion strength is approximatively 150 equivalent tons of TNT, and the surroundings are contaminated with approximatively ten grams of fission products (and the dispersed uranium fuel).

The mechanical and thermal hydraulics calculations are completed using coupled three-dimensional heat propagation and one-dimensional gas flow models. The mechanical characteristics of the composite coated particle fuel are calculated in the framework of a specially developed model. This set of tools allows a precise mechanical description of the core. According to the modeling performed, the basic version of the core (100KW of electric power) is feasible with today's technologies.

NOMENCLATURE

CEA	= Commissariat à l'Energie Atomique
OPUS	= Optimized Unit for Spacecraft
BISO	= Bistructural Isotropic (coated fuel particle)
GBR4	= Gas-Cooled Breeder Reactor 4
NPS	= Nuclear Power System
EFPD	= Equivalent Full Power Day
k_∞	= infinite medium multiplication constant
k_{eff}	= effective multiplication constant
$\Delta\rho_{BU}$	= burn-up reactivity decreasing (pcm/day)
$\alpha_{Doppler}$	= Doppler reactivity feedback (pcm/K)
β_{eff}	= delayed neutrons reactivity fraction (pcm)
L^2	= migration area (m^2)
B^2	= geometric buckling (m^{-2})
α_T	= temperature feedback coefficient (pcm/K)
Λ	= mean generation time (s)
V_{fuel}	= volume of the fuel (m^3)
ρ	= fuel density, ($kg{\cdot}m^{-3}$)
C_p	= fuel specific heat (J/kg)
Δk_0	= positive reactivity after immersion
$P(t)$, $E(t)$	= power density and energy released during the accident, ($W{\cdot}m^{-3}$, $J{\cdot}m^{-3}$)

ACKNOWLEDGMENTS

We would like to thank our colleagues and students, who participated in this project, for fruitful and enlightening discussions.

REFERENCES

1. X. RAEPSAET and S. Pascal, "Neutronic and Mechanical design of the reactor core of the OPUS system", *Proceeding of ICAPP 2007*, Nice, 2007.
2. R. SANCHEZ et al., "APOLLO2 Twelve Years Later", *Mathematics and Computation, Reactor Physics and Environmental Analysis in Nuclear Applications*, Madrid, September, 1999.
3. P. BELIER et al, "*APOLLO2 Reference Guide*", CEA-R-08-4404 (2008) .
4. A.J. KONING et al. "The JEFF evaluated data project", *Proceedings of the International Conference on Nuclear Data for Science and Technology*, Nice, 2007.
5. O. PETIT et al, "TRIPOLI-4 version 4 User Guide", CEA-R-6169 (2008).
6. J.C. TRAMA et al, "New features of TRIPOLI-4 version 5", *Proceedings of the ICRS-RPSD conference, Pine Mountain*, GA, USA, April 2008.
7. M.B. CHADWICK et al. " ENDF/B-VII.0: Next Generation Evaluated Nuclear Data Library for Nuclear Science and Technology", *Nuclear Data Sheets* **107**, 2931–3060 (2006)
8. J.-P. CATANI, "Evaluation des risques de mission", *CCT CNES "Energie de bord"*, Toulouse, France (2007).
9. W.A. DEER, R.A. Howie and J. Zussman "An introduction to the rock-forming minerals (2nd ed.)" Harlow, Longman (1992) .
10. H. GOLDENBERG and M. A. Tranter, "Heat flow in an infinite medium heated by a sphere", *Brit. J. Appl. Phys.* **3**, 296 (1952).
11. E. STUDER et al, "CAST3M/ARCTURUS: A coupled heat transfer CFD codefor Thermal-hydraulics analyses of Gas-cooled Reactors", *Proceedings of the NURETH-11 conference*, Avignon, France (2005).
12. E. HERVE and A. Zaoui, "'N-layered inclusion-based micromechanical modeling", *International Journal of Engineering Science*, **31**, 1-10 (1993).
13. E. HERVE, "Thermal and thermoelastic behaviour of multiply coated inclusion-reinforced composites", *International Journal of Solids and Structures*, **39**, 1041-1058 (2002).
14. S. PASCAL, "Change-scale modeling of the thermomechanical behaviour of particle-based nuclear fuel assemblies", *Proc. of the 18th international conference on Structural Mechanics in Reactor Technology*, Atomic Energy Press, Beijing, China (2005).
15. D.G. MARTIN, "The thermal expansion of solid UO2 and (U,Pu) mixed oxides: a review and recommendations", *Journal of Nuclear Materials*, **152**, 94-101 (1988).
16. D.G. MARTIN, "The elastic constants of polycrystalline UO2 and (U,Pu) mixed oxides: a review and recommendations", High Temps – High Press, **21**, 3-24 (1989).
17. P.G. LUCUTA, H. Matzke and I.J. Hastings, "A pragmatic approach to modeling the thermal conductivity of irradiated UO2 fuel: review and recommendations", *Journal of Nuclear Materials*, **232**, 166-180 (1996).
18. S. HISHIYAMA, T.D. Burchell, J.P. Strizak and M. Eto, "The effect of high fluence neutron irradiation on a fine-grained isotropic nuclear graphite", *Journal of Nuclear Materials*, **230**, 1-7 (1996).
19. M. PELLETIE, H. Nabielek, T. Abram and D.G. Martin, "HTR-F Project: selection of properties and models for the coated particle – PyC and SiC", CEA's internal report, NT SESC/LSC 03-028 (2003).